Hybrid UAV Attitude Control using INDI and Dynamic Tilt-Twist

Lars F.A. Dellemann and Christophe De Wagter*
Delft University of Technology, Micro Air Vehicle Lab, Kluyverweg 1, 2629HS Delft, the Netherlands

ABSTRACT

The increased search for the performance of Unmanned Aerial Vehicles (UAVs) has led to an interest in hybrid concepts like the tail-sitter UAV. A tail-sitter UAV is capable of combining vertical take-offs and landings (VTOL) with efficient long-endurance forward flights. During hover, the wings do not provide lift but instead act as disturbance and limit the yaw response. Attitude control based on direct quaternion feedback does not take the differences in reaction speed for the three axes into account. Tilt-twist control has been proposed to overcome this problem as it splits the faster tilt (pitch and roll) from the slower and less important twist (yaw) and is successfully applied to quadrotor control. This paper proposes a novel tilt-twist controller based on Incremental Nonlinear Dynamic Inversion (INDI). But in tail-sitter UAVs, the lift vector can differ a lot from the tilt angle, especially when partly or fully transitioned to forward flight. To address this, a dynamic tilt-twist controller is proposed that redefines the twist according to the transition angle. Simulations and test flight tests are performed with the NederDrone hybrid tail-sitter to show the increased performance.

1 INTRODUCTION

The market for unmanned aerial vehicles is increasing [1]. Due to the development of small processors, UAVs became widely available for the public [2]. Many companies are currently developing UAVs for various purposes [3] [4]. The reasons to use this type of aircraft are their low cost, high maneuverability, and ease of use. Quadcopters can perform VTOL but have limited flight endurance. Fixed-wing UAVs can cover larger distances than quadcopters but are not able to hover. A solution to achieve both is to use a hybrid UAV (Figure 1).

The most common hybrid UAV types are tilt-rotors [5], tilt-wings [6], tail-sitters [7] and quadplanes [8]. Both the tilt-rotors and tilt-wings have components that can rotate during the transition between hover and forward flight. A quadplane uses different actuators for hover and forward flight. A tail-sitter uses the same actuators in both flight phases and rotates the entire body of the aircraft. One of the challenges with this type of UAV is the controllability during the landing phase, especially in turbulence [9]. During hover, some of the actuators become less efficient while the wings create important perturbing forces in turbulent or hard wind.

*Email address(es): c.dewagter@tudelft.nl

Figure 1: The NederDrone, capable of performing VTOL. The tail-sitter has 20 actuators (12 motors and 8 elevons) and the energy is stored in a hydrogen tank.

1.1 NederDrone

The tail-sitter used for this project is the NederDrone [7], shown in Figure 1. The NederDrone has two wings that carry twelve engines and hold eight elevons. The twelve engines are all used during hover, but only four are used during forward flight. One characteristic is that this UAV can achieve much larger roll moments than pitch moments, and even smaller yaw moments while the yaw also experiences a lot of aerodynamic damping from the wings.

Simple quaternion control finds the shortest rotation between the current attitude and desired attitude. It then assumes that all three axes can perform the desired rotation at the same time. In hybrid aircraft like the Nederdrone where not every axis is as fast, this results in either undesired rotations or slowing down the fast axes to match the slowest. Both options are undesirable. Tilt-twist control was proposed to address this problem by splitting the tilt error (controlled by the faster pitch en roll rotations) and the twist error (controlled by the slower yaw axis) [10]. But this work used a classical controller.

Recent advances in control have shown the benefits of sensor-based approaches like Incremental Non-linear Dynamic Inversion (INDI) [11]. But INDI assumes that all rotations can be executed at the same time and that the control

demand can be met by the actuators. In hybrid aircraft such as the Nederdrone, which fly in harsh weather conditions, this is not the case.

This paper, therefore, proposes a combination of the tilt-twist method and INDI control, called the dynamic tilt-twist.

In Section 2 the theory behind the feedback error is given for quaternion, tilt-twist, and dynamic tilt-twist. Section 3 describes the methodology and results for the simulation and real-life test. Conclusions are drawn in Section 4.

2 METHOD

2.1 Axis definition

An axis system uses a body-fixed system, where the z-axis is parallel to the gravitational force during hover when the pitch and roll angles are zero. The x-axis goes through the belly of the UAV and the y-axis through the right wing (see Figure 2). In forward flight, the x-axis thereby becomes perpendicular to the gravitational force.

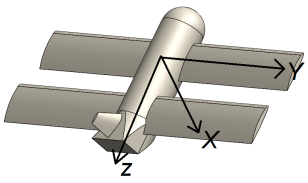

Figure 2: Body-fixed axis definition. If the pitch and roll angles are 0 degrees, the z-axis is parallel to the gravitational force vector.

2.2 Quaternion

The quaternions describe the transition of the attitude in one single rotation [12], with a rotation η and a three-dimensional unit vector component $\boldsymbol{r}$ as in

$$\boldsymbol{q} = \begin{bmatrix} \cos(\frac{\eta}{2}) \\ \boldsymbol{r}\sin(\frac{\eta}{2}) \end{bmatrix} = \begin{bmatrix} q_i & q_x & q_y & q_z \end{bmatrix}^\top \tag{1}$$

The current attitude is defined as

$$\boldsymbol{q}_c = \begin{bmatrix} q_{ci} \\ q_{cx} \\ q_{cy} \\ q_{cz} \end{bmatrix} \tag{2}$$

and the desired attitude (input) is

$$\boldsymbol{q}_d = \begin{bmatrix} q_{di} \\ q_{dx} \\ q_{dy} \\ q_{dz} \end{bmatrix} \tag{3}$$

The attitude error then becomes

$$\boldsymbol{q}_{err} = \boldsymbol{q}_d \otimes \boldsymbol{q}_c^{-1} \tag{4}$$

$$\boldsymbol{q}_{err} = \begin{bmatrix} q_{err1} \\ q_{err2} \\ q_{err3} \\ q_{err4} \end{bmatrix} = \begin{bmatrix} q_{d0} & q_{d1} & q_{d2} & q_{d3} \\ -q_{d1} & q_{d0} & q_{d3} & -q_{d2} \\ -q_{d2} & -q_{d3} & q_{d0} & q_{d1} \\ -q_{d3} & q_{d2} & q_{d1} & q_{d0} \end{bmatrix} \boldsymbol{q}_c \tag{5}$$

The controller then sends the errors in x-, y- and z-axis to the respective actuators through a PD reference generator. δ_a, δ_e and δ_r represent the aileron deflection, elevator deflection and rudder deflection respectively.

$$\delta_a = -2(k_p q_{err_2} + k_d \dot{q}_{err_2}) \tag{6}$$

$$\delta_e = -2(k_p q_{err_3} + k_d \dot{q}_{err_3}) \tag{7}$$

$$\delta_r = -2(k_p q_{err_4} + k_d \dot{q}_{err_4}) \tag{8}$$

If not all axes respond at the same speed, this results in undesired intermediate thrust vectors which disturb the position control in the position control loop.

2.3 Tilt-Twist

In hover, the two rotation angles that influence the position control are the pitch and roll. This is referred to as the tilt angle. The remaining angle is then called twist. For the Nederdrone, the tilt angles are much faster in response time than the twist since the large wings dampen the turn rate around the z-axis a lot and the torque difference of the hover motors is limited. In the presence of turbulence, the twist can even get saturated.

To address this, the tilt should be treated separately from the twist such that they can have differences in response speed. This is described as tilt-twist control [10].

2.3.1 Tilt error

The first part of the tilt-twist method consists in calculating the tilt error. The error is calculated using the rotation matrices to align the current frame with the desired frame

$$\boldsymbol{R}(\boldsymbol{q}) = \begin{bmatrix} q_i^2+q_x^2-q_y^2-q_z^2 & 2(q_x q_y+q_z q_i) & 2(q_x q_z-q_y q_i) \\ 2(q_x q_y-q_z q_i) & q_i^2-q_x^2+q_y^2-q_z^2 & 2(q_y q_z+q_x q_i) \\ 2(q_x q_z+q_y q_i) & 2(q_y q_z-q_x q_i) & q_i^2-q_x^2-q_y^2+q_z^2 \end{bmatrix} \tag{9}$$

Rotation matrices for both the current ($\boldsymbol{R}_c$) and the desired ($\boldsymbol{R}_d$) attitudes are computed as

$$\boldsymbol{R}_d = \boldsymbol{R}(\boldsymbol{q}_d) \quad \boldsymbol{R}_c = \boldsymbol{R}(\boldsymbol{q}_c) \tag{10}$$

The total tilt error can be defined as the shortest rotation between the actual and desired z-axis as illustrated in Figure 3. Note that the axis definition [10] differs from the one used in this work.

$$\boldsymbol{R}_d = \boldsymbol{R}_{err}\boldsymbol{R}_c \tag{11}$$

Equation 11 can be rewritten as

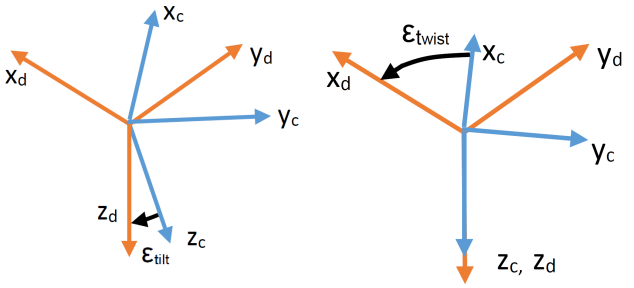

Figure 3: The tilt and twist error definitions. In the tilt plot, the pitch error is 10°, the roll error 5° and the yaw error is 60°. In the twist plot, the pitch error is 0° and the roll error 0°.

$$\boldsymbol{R}_{err} = \boldsymbol{R}_d \boldsymbol{R}_c^\top = \begin{bmatrix} r_{1,1} & r_{1,2} & r_{1,3} \\ r_{2,1} & r_{2,2} & r_{2,3} \\ r_{3,1} & r_{3,2} & r_{3,3} \end{bmatrix} \tag{12}$$

The third row component of matrix $\boldsymbol{R}_{err}$ then provides the tilt error. The x-component of the tilt error is given by

$$Tilt\ error_1 \triangleq \varepsilon_x = -atan2(r_{3,2}, r_{3,3}) \tag{13}$$

where $atan2$ is the inverse tangent. The y-component is given by

$$Tilt\ error_2 \triangleq \varepsilon_y = atan2(r_{3,1}, r_{3,3}) \tag{14}$$

2.3.2 Twist error

The twist error is calculated as the angle error around the body fixed z-axis. An intermediate coordinate frame is defined that reflects the current attitude after removing the tilt error. This is achieved by using the rotation matrices

$$\boldsymbol{R}_d = \begin{bmatrix} \boldsymbol{r}_{d1} \\ \boldsymbol{r}_{d2} \\ \boldsymbol{r}_{d3} \end{bmatrix} \quad \boldsymbol{R}_c = \begin{bmatrix} \boldsymbol{r}_{c1} \\ \boldsymbol{r}_{c2} \\ \boldsymbol{r}_{c3} \end{bmatrix} \tag{15}$$

where the elements $\boldsymbol{r}$ represent vectors with the body axes expressed in the vehicle frame. The total tilt error then becomes

$$Tilt\ error \triangleq \varepsilon_{tilt} = \cos^{-1}\left(\boldsymbol{r}_{d3}^\top \cdot \boldsymbol{r}_{c3}^\top\right) \tag{16}$$

Next, the unit length axis is defined as

$$k = \frac{\boldsymbol{r}_{c3}^\top \times \boldsymbol{r}_{d3}^\top}{|\boldsymbol{r}_{c3}^\top \times \boldsymbol{r}_{d3}^\top|} \tag{17}$$

As the rotation needs to happen in the vehicle frame, the unit vector k is rotated to the vehicle frame

$$\boldsymbol{v}^b = \boldsymbol{R}_c k = \begin{bmatrix} v_x^b \\ v_y^b \\ v_z^b \end{bmatrix} \tag{18}$$

Then, a rotation matrix is defined which rotates a vector around a vector with a given angle. This is accomplished by using the Rodrigues rotation formula[1], where the angle is ε_{tilt} and the vector is $\boldsymbol{v}^b$. The rotation becomes

$$\boldsymbol{R}_v = \begin{cases} \boldsymbol{I}, & \varepsilon_{tilt} = 0 \\ \boldsymbol{I} - \boldsymbol{v}\sin(\varepsilon_{tilt}) + \boldsymbol{v}^2[1 - \cos(\varepsilon_{tilt})], & \varepsilon_{tilt} \neq 0 \end{cases} \tag{19}$$

where

$$\boldsymbol{v} = \begin{bmatrix} 0 & -v_z^b & v_y^b \\ v_z^b & 0 & -v_x^b \\ -v_y^b & v_x^b & 0 \end{bmatrix} \tag{20}$$

The error is then expressed in the body frame by multiplying $\boldsymbol{R}_v$ with the rotation matrix of the current attitude of the UAV $\boldsymbol{R}_c$

$$\boldsymbol{R}_p = \boldsymbol{R}_v^\top \boldsymbol{R}_c \tag{21}$$

where

$$\boldsymbol{R}_p = \begin{bmatrix} \boldsymbol{r}_{p1} \\ \boldsymbol{r}_{p2} \\ \boldsymbol{r}_{p3} \end{bmatrix} \tag{22}$$

The absolute twist error, illustrated in Figure 3, can be found using the x-components of $\boldsymbol{R}_p$ and $\boldsymbol{R}_d$ with

$$\varepsilon_{twist} = \cos^{-1}\left(\boldsymbol{r}_{p1}^\top \cdot \boldsymbol{r}_{d1}^\top\right) \tag{23}$$

To determine the sign of the twist error, the y component of $\boldsymbol{R}_p$ is used in

$$\varepsilon_{sign} = \cos^{-1}\left(\boldsymbol{r}_{p2}^\top \cdot \boldsymbol{r}_{d1}^\top\right) \tag{24}$$

Finally, when ε_{twist} is above 90°, the sign of the twist error becomes inverted and is corrected with

$$Twist\ error \triangleq \varepsilon_z = \begin{cases} \varepsilon_{twist}, & \varepsilon_{sign} \leq \frac{\pi}{2} \\ -\varepsilon_{twist}, & \varepsilon_{sign} > \frac{\pi}{2} \end{cases} \tag{25}$$

Together, the total feedback error is set as

$$Feedback\ error \triangleq \boldsymbol{\varepsilon} = \begin{bmatrix} \varepsilon_x \\ \varepsilon_y \\ \varepsilon_z \end{bmatrix} \tag{26}$$

The PD reference generator in the total INDI controller [11] is then written as

$$\delta_a = k_p \varepsilon_x - k_d \dot{\varepsilon}_x \tag{27}$$

$$\delta_e = k_p \varepsilon_y - k_d \dot{\varepsilon}_y \tag{28}$$

$$\delta_r = k_p \varepsilon_z - k_d \dot{\varepsilon}_z \tag{29}$$

By using gains that result in slower reaction on the twist, time-separation of tilt and twist is achieved.

[1] https://mathworld.wolfram.com/RodriguesRotationFormula.html, Oct 2020

2.4 Comparison of quaternion and tilt-twist

Figure 4 illustrates the difference between quaternion feedback tilt-twist feedback on a purely kinematic model with rate-limited yaw control. A simulation is performed where there is a small pitch and roll error and a large yaw error. The rate-limited yaw takes more time to converge than pitch and roll, but more importantly, in quaternion control, the pitch and roll only reach their desired values when the yaw has converged. Since errors in tilt also affect the position control in the outer loop, this will result in larger position errors for the simple quaternion control. The tilt-twist method addresses this problem.

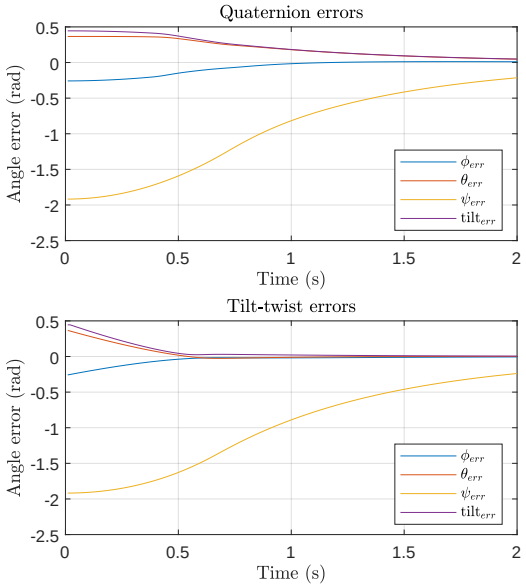

Figure 4: Error handling comparison between tilt-twist and quaternion feedback, in Euler angles. The tilt error is also shown, which is linked to the thrust vector.

2.5 Dynamic Tilt-Twist

In the tilt-twist method, the twist component is always measured around the body fixed z-axis. This is ideal in quadrotors but in hybrid aircraft such as the Nederdrone, when there is wind, the UAV hovers at pitch angles of up to 50 to 70 degrees nose down from hover. In that case, the body tilt axis does not correspond to the lift vector anymore. The goal of tilt-twist—to have the actual lift vector make the shortest rotation—thereby becomes invalid. Moreover, in these conditions, the additional airflow over the main wing, fortunately, improves the achievable turn rate around the x-axis.

To address these conditions, a dynamic tilt-twist controller is introduced. The tilt axis is redefined to be parallel with the gravitational vector. To align the twist vector with the gravitational vector the rotational matrix $\boldsymbol{R}_a$ is used which includes the pitch (θ) and roll (ϕ) angle:

$$\boldsymbol{R}_a(\theta,\phi) = \begin{bmatrix} \cos-\theta & \sin-\theta\sin-\phi & \sin-\theta\cos-\phi \\ 0 & \cos-\phi & -\sin-\phi \\ -\sin-\theta & \cos-\theta\sin-\phi & \cos-\theta\cos-\phi \end{bmatrix} \tag{30}$$

Thereby, the rotation matrices from Equation 10 are redefined as

$$\boldsymbol{R}_d = \boldsymbol{R}_a\boldsymbol{R}(\boldsymbol{q}_d) \tag{31}$$

$$\boldsymbol{R}_c = \boldsymbol{R}_a\boldsymbol{R}(\boldsymbol{q}_c) \tag{32}$$

Then the same tilt-twist controller is used as in the previous section, except for the last step where the actuator deflections need to be compensated again for the dynamic tilt angle using the inverse rotation $\boldsymbol{R}_a^{-1}$

$$Feedback\ error \triangleq \boldsymbol{\varepsilon} = \begin{bmatrix} \varepsilon_x \\ \varepsilon_y \\ \varepsilon_z \end{bmatrix} \boldsymbol{R}_a^{-1} \tag{33}$$

3 SIMULATION AND FLIGHT TEST

The paparazzi autopilot system [13] and simulator with a Nederdrone model are used to perform the simulations and flight tests. The controller is an INDI controller [14] with a modified linear control input. Three different reference generators are compared: quaternion feedback, tilt-twist, and dynamic tilt-twist. The setup is identical for the simulations and the flight test. The tests consisted of flying the Nederdrone back and forth between two waypoints where it needed to hover for three seconds. To induce errors in yaw and highlight the differences in the different controllers, a heading offset ψ_{change} is artificially added each time the Nederdrone leaves a waypoint. Finally, the trajectory errors are compared since optimizing trajectory tracking is the overarching goal.

3.1 Results

3.1.1 Simulation

Before the flight tests, the different types of feedback errors were tested in a simulation. The same controller settings were used for the flight test. The heading offset (ψ_{change}) during the simulation was set to 160°. The simulation results are presented in Figure 5. During the simulation, no wind was taken into account. It can be seen that the quaternion feedback resulted in irregular behavior. The tilt-twist and dynamic tilt-twist methods were much more consistent.

3.1.2 Flight test

Flight tests in windy conditions were performed with the Nederdrone on a path (orange) at about 50° angle with the wind. The heading offset, ψ_{change}, was set to jumps of 45° for the tilt-twist controllers but due to stability issues only to 30° for the quaternion controller (See Figure 6). Higher heading offsets could result in an unsafe flight when the quaternion feedback controller is used.

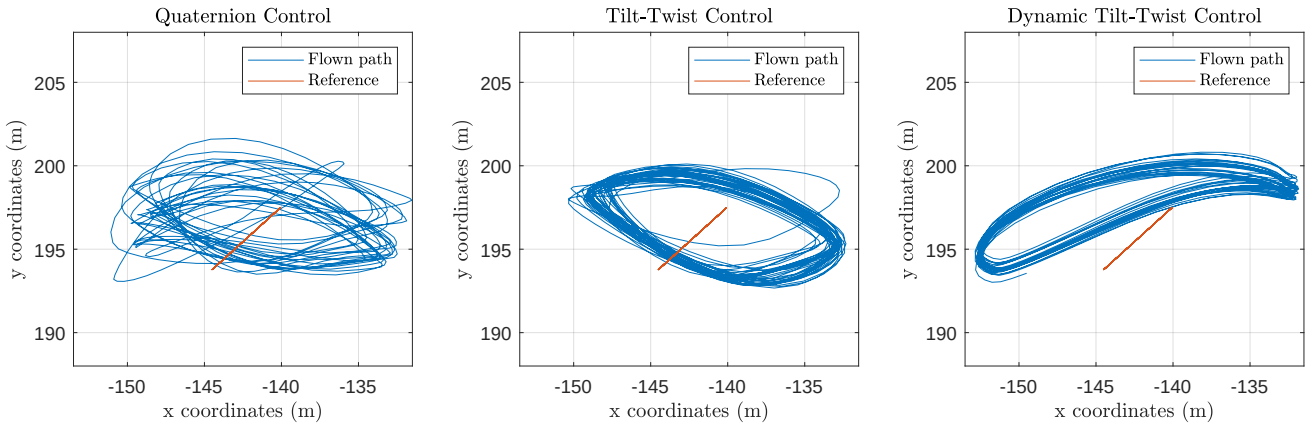

Figure 5: Flight paths during simulation (quaternion, tilt-twist, dynamic tilt-twist). The quaternion feedback method had problems with handling the yaw angle error. Both the tilt-twist and the dynamic tilt-twist method showed more stable behavior.

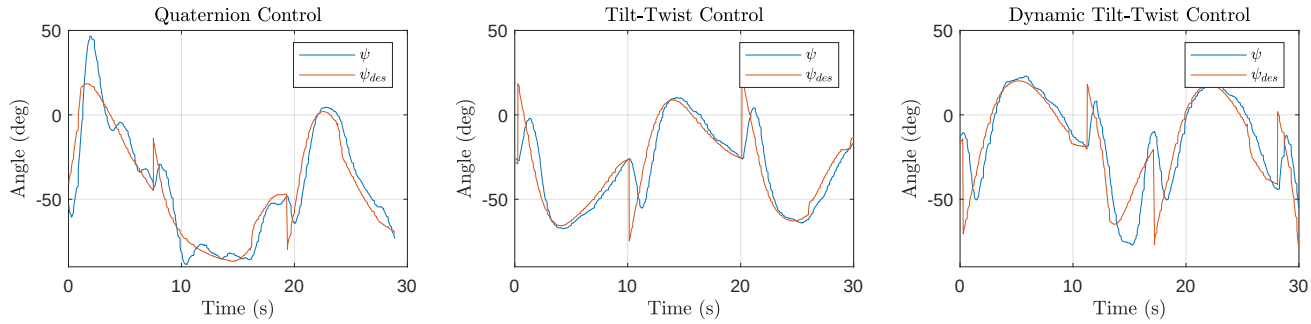

Figure 6: Commanded and actual heading angle ψ where the artificially added jump in commanded heading simulates situations where a large heading error is present.

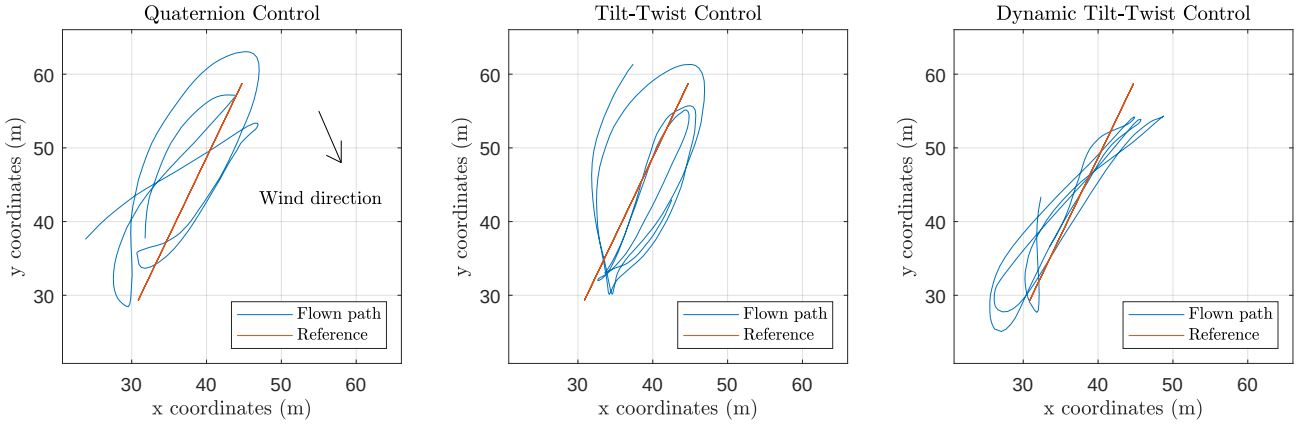

Figure 7: Flown path during flight test, the wind conditions were equal for all flights

The flight paths of the Nederdrone can be seen when using the three controllers in Figure 7. Table 1 shows the numeric comparison of the achieved position accuracy as measured during the same flight in the same conditions by switching the controller in flight. The quaternion controller shows some irregular behavior that depends on the difficulty to reach the desired yaw angle. The tilt-twist method is shown to yield more consistent results than the quaternion controller in the same conditions. Finally, the dynamic tilt-twist method improves the behavior even further.

Table 1: Test results, distance from the reference line.

	Average distance (m)
Quaternion	3.27
Tilt-twist	2.74
Dynamic tilt-twist	2.08

4 CONCLUSION

This paper presented the combination of INDI control with tilt-twist control and proposed an improvement for hybrid aircraft where the lift vector does not always correspond to the thrust vector, namely the dynamic tilt-twist method. The simulation and the flight test demonstrated that the quaternion feedback method had problems following the required path, whereas the tilt-twist method showed some improvements and the dynamic tilt-twist showed the best results. The dynamic tilt-twist method is suitable for tail-sitters that vary their pitch and roll angles during hover and experience yaw/position control problems.

ACKNOWLEDGMENTS

The authors would like to thank the Nederdrone team and sponsors for their support.

REFERENCES

[1] L. Canetta, G. Mattei, and A. Guanziroli. Exploring commercial UAV market evolution from customer requirements elicitation to collaborative supply network management. In *2017 International Conference on Engineering, Technology and Innovation (ICE/ITMC)*, pages 1016–1022, June 2017.

[2] S. Bouabdallah, P. Murrieri, and R. Siegwart. Design and control of an indoor micro quadrotor. In *IEEE International Conference on Robotics and Automation, 2004. Proceedings. ICRA '04. 2004*, volume 5, pages 4393–4398 Vol.5, 2004.

[3] A. Saha, A. Kumar, and A. K. Sahu. FPV drone with GPS used for surveillance in remote areas. In *2017 Third International Conference on Research in Computational Intelligence and Communication Networks (ICRCICN)*, pages 62–67, 2017.

[4] K. Feng, W. Li, S. Ge, and F. Pan. Packages delivery based on marker detection for UAVs. In *2020 Chinese Control And Decision Conference (CCDC)*, pages 2094–2099, Aug 2020.

[5] G. Flores and R. Lozano. Transition flight control of the quad-tilting rotor convertible MAV. In *2013 International Conference on Unmanned Aircraft Systems (ICUAS)*, pages 789–794, 2013.

[6] K. Muraoka, N. Okada, and D. Kubo. Quad Tilt Wing VTOL UAV: Aerodynamic Characteristics and Prototype Flight. In *AIAA Infotech@Aerospace Conference*, 2012.

[7] C. De Wagter, B. Remes, R. Ruijsink, F. van Tienen, and E. van der Horst. Design and Testing of a Vertical Take-Off and Landing UAV Optimized for Carrying a Hydrogen Fuel Cell with a Pressure Tank. *Unmanned Systems*, 08(04):279–285, 2020.

[8] A. Wang and T. Chan. Estimation of Drag for a Quad-Plane Hybrid Unmanned Aerial Vehicle. In *2017 AIAA Student Conference Region VII-AUAt: Melbourne, Australia*, 11 2017.

[9] C. De Wagter, R. Ruijsink, E. Smeur, K. van Hecke, F. van Tienen, E. van der Horst, and B. Remes. Design, control, and visual navigation of the DelftaCopter VTOL tail-sitter UAV. *Journal of Field Robotics*, pages 937–960, 2018.

[10] T. Matsumoto, K. Kita, R. Suzuki, A. Oosedo, K. Go, A. Konno Y. Hoshino, and M. Uchiyam. A Hovering Control Strategy for a Tail-Sitter VTOL UAV that Increases Stability Against Large Disturbance. In *2010 IEEE International Conference on Robotics and Automation*, Anchorage, AK, USA, May 2010. IEEE.

[11] S. Sieberling, Q. P. Chu, and J. A. Mulder. Robust Flight Control Using Incremental Nonlinear Dynamic Inversion and Angular Acceleration Prediction. *Journal of Guidance, Control, and Dynamics*, 33(6):1732–1742, 2010.

[12] J. Cariño, H. Abaunza, and P. Castillo. Quadrotor quaternion control. In *2015 International Conference on Unmanned Aircraft Systems (ICUAS)*, pages 825–831, June 2015.

[13] Gautier Hattenberger, Murat Bronz, and Michel Gorraz. Using the Paparazzi UAV System for Scientific Research. In *IMAV 2014, International Micro Air Vehicle Conference and Competition 2014*, pages 247–252, Delft, Netherlands, August 2014. IMAV.

[14] E. Smeur. *Incremental Control of Hybrid Micro Air Vehicles*. PhD thesis, Delft University of Technology, 2018.